JOURNAL OF AGRICULTURAL AND FOOD CHEMISTRY

REVIEWS

A Review on Spectrophotometric Methods for Measuring the Monophenolase and Diphenolase Activities of Tyrosinase

F. GARCÍA-MOLINA,[†] J. L. MUÑOZ,[†] R. VARÓN,[‡] J. N. RODRÍGUEZ-LÓPEZ,[†] F. GARCÍA-CÁNOVAS,*[,†] AND J. TUDELA[†]

GENZ: Grupo de Investigación de Enzimología, Departamento de Bioquímica y Biología Molecular-A, Facultad de Biología, Universidad de Murcia, E-30100 Espinardo, Murcia, Spain, and Departamento de Química-Física, Escuela Politécnica Superior, Universidad de Castilla la Mancha, Avda. España s/n, Campus Universitario, E-02071 Albacete, Spain

Tyrosinase is a copper enzyme with broad substrate specifity toward a lot of phenols with different biotechnological applications. The availability of quick and reliable measurement methods of the enzymatic activity of tyrosinase is of outstanding interest. A series of spectrophotometric methods for determining the monophenolase and diphenolase activities of tyrosinase are discussed. The product of both reactions is the *o*-quinone of the corresponding monophenol/diphenol. According to the stability and properties of the *o*-quinone, the substrate is classified as four substrate types. For each of these substrate types, we indicate the best method for measuring diphenolase activity (among eight methods) and, when applicable, for measuring monophenolase activity (among four methods). The analytical and numerical solutions to the system of differential equations corresponding to the reaction mechanism of each case confirm the underlying validity of the different spectrophotometric methods proposed for the kinetic characterization of tyrosinase in its action on different substrates.

KEYWORDS: Spectrophotometric methods; monophenolase; diphenolase; polyphenol oxidase; tyrosinase

INTRODUCTION

Tyrosinase or polyphenol oxidase (PPO) (monophenol, *o*-diphenol: O_2 oxidoreductase, EC 1.14.18.1), is an enzyme with a binuclear copper center that catalyzes two different reactions, in both of which it uses molecular oxygen. These reactions are the orthohydroxylation of monophenols (M) to *o*-diphenols (D) (monophenolase activity) and the oxidation of *o*-diphenols to their *o*-quinones (Q) (diphenolase activity) (*1*, *2*).

The active site of the enzyme contains a pair of antiferromagnetically coupled copper(II) ions or T3 center. Three forms exist in the catalytic cycle: "met", "deoxy", and "oxy" (*2*). The structure of mushroom tyrosinase is not known, but evolutionary correlations and spectroscopic similarities (*3*, *4*) with two related proteins containing the same type-3 copper that have been structurally characterized, namely, hemocyanin (*5*, *6*) and catechol oxidase (*7*), suggest a common active site, in which six histidine ligands are bound to the pair of copper ions (*8*). The crystal structure of a tyrosinase from *Streptomyces* bound to a "caddie protein" has been resolved (*9*).

Several reviews on PPO have recently been published, including plant PPO (*10*) and mushroom PPO with inhibitors (*11*, *12*), and another on potential applications in bioengineering and biotechnology (*13*). Indeed, since 1994 hundreds of papers dealing with plant and fungal PPO have been published. Many methods have been used to measure enzyme activity, although many pitfalls exist in this respect, basically, we think, because of the reactions that the product of the enzymatic action (*o*-quinone) undergo with the original substrate or with nucleophilic reagents (*14*).

PPO is an enzyme with a wide range of substrate specificity, which has led to many methods being proposed to measure its activity: radiometric (*15*, *16*), electrometric (*17*, *18*), chronometric (*19*, *20*) and, especially spectrophotometric (*21*–*44*), which are fast and affordable by most laboratories. A review about some of the methods used to measure the different enzymes involved in melanogenesis has been published (*45*).

PPO uses molecular oxygen to hydroxylate monophenols to *o*-diphenols, which are then oxidized to their corresponding *o*-quinone. This *o*-quinone, in turn, takes part in a series of

* Corresponding author. Fax: +34 968 363963. E-mail address: canovasf@um.es. URL: http://www.um.es/genz.
[†] Universidad de Murcia.
[‡] Universidad de Castilla la Mancha.

10.1021/jf0712301 CCC: $37.00
Published on Web 10/25/2007

Scheme 1. Basic Reaction Mechanism of PPO on *o*-Diphenols[a]

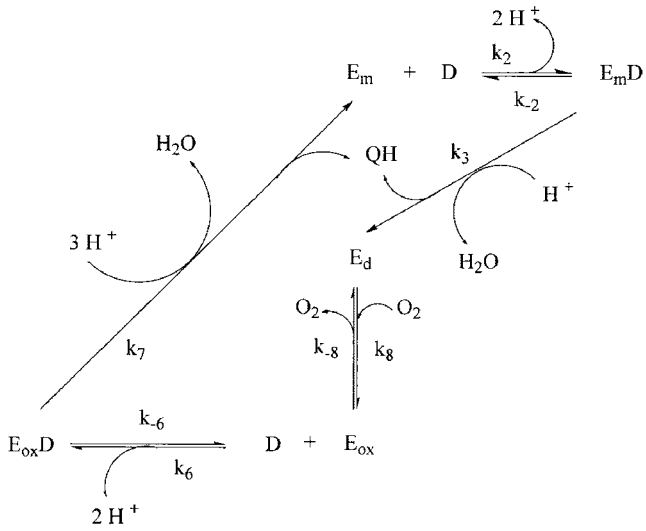

[a] Q evolves through the reactions indicated in **Scheme 2**.

chemical reactions and finally polymerizes (*40*). Although most quinones are unstable, if some colored intermediary accumulates in the medium, that is, if it evolves slowly, it can be measured spectrophotometrically. Moreover, quinones can react with nucleophilic reagents (N), which is useful for directing them toward a chromophoric product, nucleophile-quinone (NQ) with a given stoichiometry (*22, 24, 31–33, 35–39*).

The fact that PPO catalyzes the oxidation of its monophenol/*o*-diphenol substrates, giving rise to unstable *o*-quinones, has led some authors to propose that the best way to measure the enzymatic activity is to measure the disappearance of the monophenol or *o*-diphenol (*43*). This stems from the fact that most spectrophotometric methods proposed in the literature are based on measuring the product of the *o*-quinone as it evolves or the product of its reaction with a reagent (*21–44*). The methods used to measure the disappearance of substrate are no better than those used to measure the appearance of product in an enzymatic reaction (*46*). Furthermore, when substrate disappearance is measured at ultraviolet wavelengths, the molar absorptivity coefficients are usually high and the concentration cannot be increased much to reach PPO saturation because the phototube will not respond.

The aim of this review is to identify the best spectrophotometric method for measuring each particular type of tyrosinase substrate, which we shall group into four types. Eight methods will be proposed to measure diphenolase activities and four for measuring monophenolase activity. The kinetic basis of each method will be described, and an example of its application to a characteristic substrate of tyrosinase from each group will be given. The simulated values of the reaction rates obtained by the theoretical detection of several species will be compared with the experimental procedures described in the bibliography.

KINETIC REACTION MECHANISM OF PPO ACTIVITY

Diphenolase Activity. The kinetic mechanism of **Scheme 1** describes the turnover of the diphenolase activity of tyrosinase, based on structural and kinetic studies (*2, 37, 40, 47–49*). The native form of the enzyme is mainly as E_m, with the copper oxidized. This form binds to an *o*-diphenol molecule, forming the complex E_mD; the oxidized form of the *o*-diphenol is released in the form of *o*-quinone and the enzyme is reduced to the deoxy form E_d, which binds to an oxygen molecule to give the species E_{ox}, which reacts again with another *o*-diphenol molecule producing the complex $E_{ox}D$. The *o*-diphenol is then oxidized to *o*-quinone, and the enzyme returns to its E_m form. The *o*-quinones formed evolve in different ways depending on their stability, and it is the way in which they evolve that is useful in the different spectrophotometric measurement methods indicated in **Scheme 2** (*26, 50*).

Monophenolase Activity. PPO turnover in monophenolase activity is more complex (**Scheme 3**). In reactions that reach the steady state, the *o*-quinone generated must evolve chemically in such a way that a given quantity of *o*-diphenol is accumulated in the medium (**Scheme 4**). The turnover of PPO acting on monophenols (if the steady state is reached) involves (according to **Scheme 3**) a hydroxylase cycle, an oxidase cycle, and a dead end, which coincide with the sequence of chemical reactions that originate from the *o*-quinone (**Scheme 4**).

Briefly, E_{ox} would start the turnover by acting on M, which is hydroxylated to generate E_mD. At this point the enzyme may oxidize D to Q, generating E_d, or release D producing E_m, which would bind with M to produce the inactive form E_mM. If *o*-quinone is unstable, as occurs in the case of *o*-dopaquinone, D is recycled to the reaction medium through intramolecular cyclization and further redox steps (*40, 50*). This would involve the transformation of E_m (which is inactive toward M) into the E_{ox} (which is active toward M) and give rise to the lag period which is a characteristic of this activity (**Schemes 3** and **4**). Another way in which *o*-diphenol can be accumulated in the reaction medium is to attack it with a nucleophilic reagent (N) generating a nucleophile-quinone (NQ) (**Schemes 3** and **4B**) (*35–37*). In both cases the system reaches the steady state. However, if the *o*-quinone is very stable or if it is reduced continuously with a reductant such as ascorbic acid (**Schemes 3** and **4C**) (*51*), the system will never reach the steady state. All this must be borne in mind when developing methods for measuring the monophenolase activity (see below).

SUGGESTED CLASSIFICATION OF THE SUBSTRATES OF TYROSINASE

Due to the wide specificity of PPO, several types of substrate can be considered according to the stability of the corresponding quinone:

S_A: Substrates Yielding Stable *o*-Quinone. The clearest example is 4-*tert*-butylcatechol (TBC) whose *o*-quinone (*o*-TBQ) is very stable. In this case, the *o*-quinone can be measured and V_0 can be calculated accurately (*44*). The diphenolase activity can be determined, but not the monophenolase activity (*52*) (see below).

S_B: Substrates Yielding a Stable Coupling Product. This is a substrate that produces a very unstable *o*-quinone but that evolves to a stable product through a first-order reaction. An example is 3,4-dihydroxymandelic acid (DOMA) whose *o*-quinone evolves to 3,4-dihydroxybenzaldehyde (DOBA) (*34*). Other examples of a type S_B substrate are L-dopa (*26*), dopamine (*27*), L-α-methylnoradrenaline (*28*), isoproterenol (*29*), epinine (*31*), and L-dopa methyl ester (*53*), whose *o*-quinone evolves to aminochrome. A kinetic analysis shows that the experimentally measurable velocity is directly related with the real enzymatic activity, V_0 in the first case (DOMA) and $V_0/2$ in all other cases. The diphenolase activity can be monitored in either of the above cases by measuring the accumulation of stable product generated. The monophenolase activity can be obtained through measuring the formation

Scheme 2. Reaction Mechanism of PPO on *o*-Diphenols, Considering the Chemical Evolution of the *o*-Quinone[a]

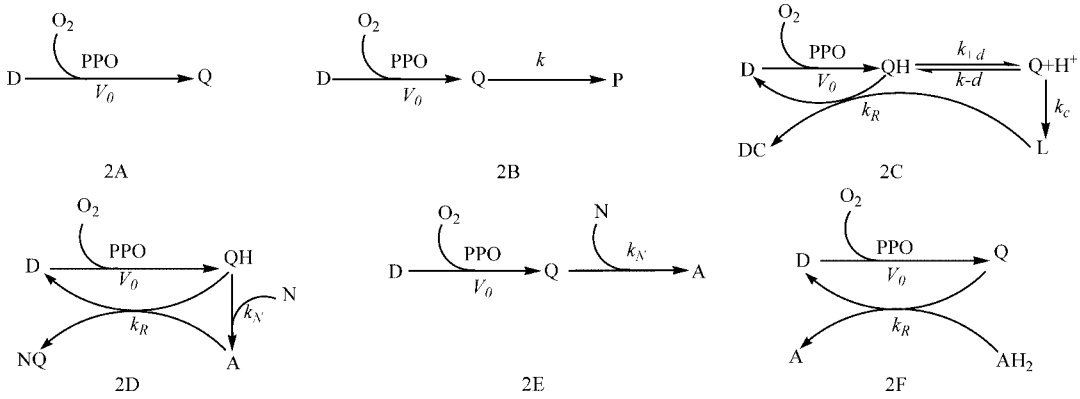

[a] Mechanism 2A, stable Q. Mechanism 2B, Q evolves toward P with a first-order reaction mechanism. Mechanism 2C, Q evolves by means of a deprotonation reaction, cyclization, and oxidation–reduction toward DC. Mechanism 2D, Q is submitted to a nucleophilic attack by N, forming NQ. Mechanism 2E, Q is attacked by L-cysteine as nucleophile, giving rise to adduct A. Mechanism 2F, Q is reduced by AH_2.

Scheme 3. Basic Mechanism of PPO Acting on Monophenols[a]

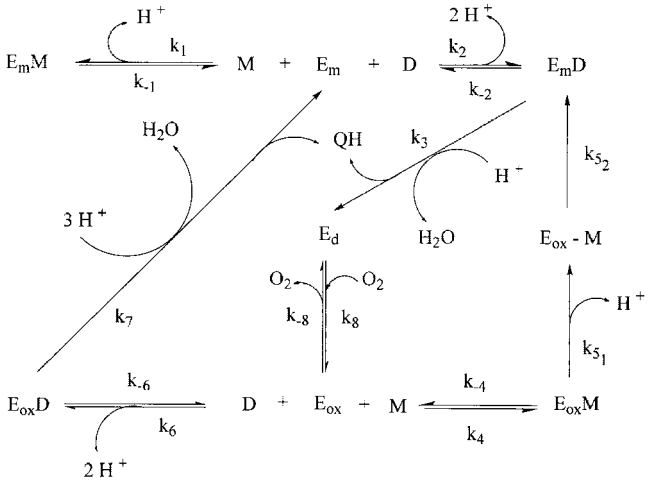

[a] Q evolves through the reactions indicated in **Scheme 4**.

Scheme 4. Mechanism of PPO Acting on M, Considering the Evolution of Q[a]

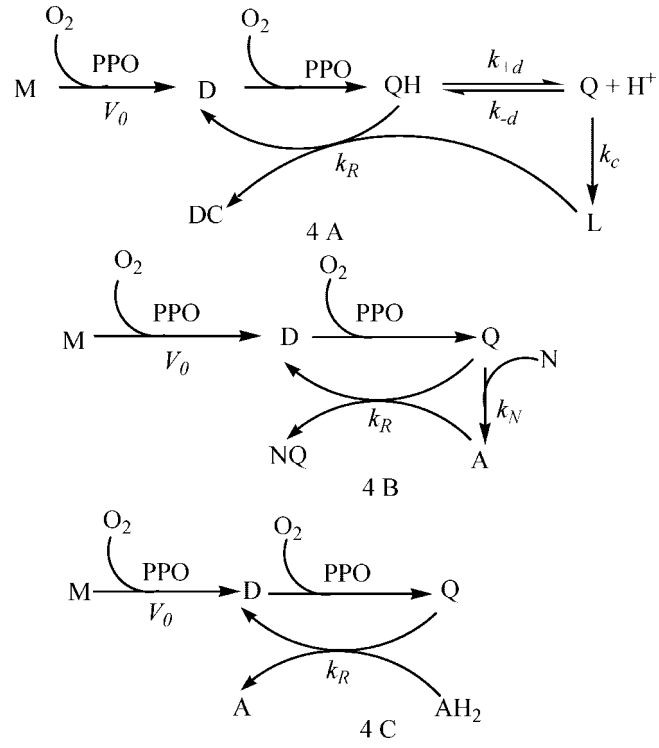

[a] Mechanism 4A, Q evolves by a deprotonation reaction, cyclization, and oxidation/reduction toward DC. Mechanism 4B, Q evolves through nucleophilic attack of N toward NQ. Mechanism 4C, Q is reduced by AH_2.

of product in the case of the monophenols corresponding to L-dopa, dopamine, and L-dopa methyl ester (L-tyrosine, tyramine, and tyrosine methyl ester, respectively) (*40*, *53*).

S_C: Substrates Yielding a Stable Nucleophile Adduct. The oxidation of this type of substrate gives rise to an unstable *o*-quinone which suffers the attack of a potent nucleophilic reagent (N) and produces a chromophoric adduct (NQ) with a clear stoichiometry. Among the nucleophilic reagents used are L-proline (Pro) (*32*), MBTH (*22*, *24*, *33*, *35*–*38*), and L-cysteine (Cys) (*39*). Kinetic analyses in the cases of Pro and MBTH show that the accumulation rate of the colored chromophore corresponds to $V_0/2$. In the case of L-cysteine, the rate is exactly that of the enzyme V_0 (see below (*39*)). When Pro or MBTH is used, the accumulation of the chromophoric product permits us to characterize the monophenolase and diphenolase activities (L-tyrosine, tyramine, 4-hydroxyphenylacetic acid, 4-hydroxyphenylpropionic acid, L-dopa, dopamine, 3,4-dihydroxyphenylacetic acid, 3,4-dihydroxyphenylpropionic acid) (*37*).

S_D: Substrates Measured through Ascorbic Acid. This is a substrate that gives rise to a very unstable *o*-quinone that evolves with no clear stoichiometry, even through MBTH attack. It can only be characterized through reduction by ascorbic acid (AH_2), either by direct means and spectrophotometrically following the disappearance of ascorbic acid (*21*, *44*) or by using chronometric methods that measure the time necessary for the ascorbic acid to be consumed due to the reaction with *o*-quinone (*19*, *20*, *23*, *44*). In this case, measurement by reference to the reduction of the *o*-quinone by ascorbic acid makes it possible to characterize the diphenolase but not the monophenolase activity (*19*, *20*, *44*, *51*).

This review will look at a total of 12 spectrophotometric methods for kinetically characterizing the activity of PPO on different types of substrate (**Table 1**) because of the interest this holds for mechanistic and comparative studies and for establishing possible structure/function relationships.

Table 1. Spectrophotometric Methods Proposed for Measuring the Diphenolase and Monophenolase Activities of Tyrosinase

	type S_A substrates	type S_B substrates	type S_C substrates	type S_D substrates
diphenolase activity	method 1	methods 2, 3	methods 4, 5	methods 6–8
monophenolase activity	method 9	method 10	method 11	method 12

MEASUREMENT METHODS

We shall look at the diphenolase activity of PPO first and then the monophenolase activity, taking into account the different types of substrate described above and following a series of steps to check the measurement methods proposed.

Step 1. Each of the spectrophotometric methods described is represented by a kinetic scheme.

Step 2. A simple kinetic analysis is carried out which describes analytically how the experimental measurement is related with the enzyme activity (V_0).

Step 3. Some of the references in which the method considered has been used experimentally are described.

Step 4. Simulated progress curves corresponding to the mechanism being studied are obtained. In each case, we obtain the initial disappearance rate of the substrates and the appearance rate of the spectrophotometrically measurable compound, showing their equivalence. The values of the corresponding rate constants used for the simulation assays are detailed in the Supporting Information.

Below, we outline the different methods proposed for characterizing the diphenolase and monophenolase activities of PPO (**Table 1**).

Diphenolase Activity. The action of PPO on *o*-diphenols is described by **Scheme 1** (*49, 50, 53, 54*). Henceforth, **Scheme 1** will be represented in simplified form in the different schemes of **Scheme 2**. Then we shall consider the different types of *o*-quinone that are generated after the action of PPO according to the type of substrate.

Method 1: S_A. Step 1. The kinetic scheme is described by **Scheme 2A**. The experimental measurement is made spectrophotometrically at the wavelength corresponding to the maximum absorbance of the *o*-quinone.

Step 2. The kinetic analysis of the mechanism indicated in **Scheme 1** provides the analytical expression for the kinetic parameter, $V_0^{D,Q}$, the initial rate of the enzyme action measuring the formation of Q is (*48*)

$$V_0^{D,Q} = \frac{V_{max}^{D,Q}[D]_0[O_2]_0}{K_s^{O_2}K_m^D + K_m^D[O_2]_0 + K_m^{O_2,D}[D]^0 + [O_2]_0[D]_0} \quad (1)$$

where

$$V_{max}^{D,Q} = 2k_{cat}^D[E]_0 \quad (2)$$

$$k_{cat}^D = \frac{k_3k_7}{k_3 + k_7} \quad (3)$$

$$K_s^{O_2} = \frac{k_{-8}}{k_8} \quad (4)$$

$$K_m^D = \frac{k_{cat}^D}{k_6} \quad (5)$$

$$K_m^{O_2,D} = \frac{k_{cat}^D}{k_8} \quad (6)$$

In the case of mushroom PPO, $K_m^{O_2,D} \ll [O_2]_0$ (*48*), so that eq 1 is simplified to:

$$V_0^{D,Q} = \frac{V_{max}^{D,Q}[D]_0}{K_m^D + [D]_0} \quad (7)$$

Step 3. The $V_0^{D,Q}$ determined can be analyzed according to eq 7, providing the kinetic constants for the enzyme acting on D. To the best of our knowledge, TBC is the only substrate of PPO that gives rise to a stable Q. The slope of the straight line obtained by measuring the absorbance at 410 nm versus *t* provides the value of $V_0^{D,Q}$, (*37, 44*).

Step 4. The simulated progress curves corresponding to the mechanism shown in **Schemes 1** and **2A**, and taking into account the values of the kinetic constants provided in the literature (*37, 48*), provide a straight line for the accumulation of Q, **Figure 1** (trace a) from which $V_0^{D,Q}$, can be obtained. Moreover, the simulation provides the values of V_0^D (initial rate obtained measuring the disappearance of D) and V_0^{D,O_2} (initial rate measuring the disappearance of O_2). Note the concordance with the values given in **Table 2**, which reflects the stoichiometry $V_0^D = 2V_0^{D,O_2} = V_0^{D,Q}$. Below, we shall show how method 1 cannot kinetically characterize the action of PPO on 4-*tert*-butylphenol (TBF) (*52*).

Method 2: S_B. The *o*-quinone generated by the action of PPO on this type of substrate is stabilized in a first-order reaction.

Step 1. The kinetic scheme corresponding to this method is described in **Scheme 2B**.

Step 2. The parameter measured is the initial velocity of the enzyme acting on the substrate (V_0). If the *o*-quinone is unstable and becomes a stable product, the quantity of matter entering the system at time *t* will be V_0t.

This matter is distributed between *o*-quinone (Q) and product (P) in such a way that

$$V_0t = [Q] + [P] \quad (8)$$

Thus, the accumulation of P with time in the steady state is

$$[P] = V_0t - [Q]_{ss} \quad (9)$$

An experimental measurement of [P] versus *t* gives to a straight line with a slope V_0, which is the parameter to be measured and which we call $V_0^{D,P}$. However, the product P accumulates in the medium with a lag, τ, that depends on the value of the first-order rate constant *k*.

When [P] = 0, extrapolation to intercept the time axis according to eq 9 gives

$$\tau = \frac{[Q]_{ss}}{V_0} \quad (10)$$

where τ is the lag period. As Q reaches the steady state, the following is fulfilled

$$\frac{d[Q]}{dt} = V_0 - k[Q]_{ss} \quad (11)$$

and so

$$[Q]_{ss} = \frac{V_0}{k} \quad (12)$$

Substituting in eq 10 gives

$$\tau = \frac{1}{k} \quad (13)$$

Step 3. This case would correspond exactly to the measurement method based on the oxidation of DOMA by PPO, in which the corresponding *o*-quinone spontaneously decarboxylates to DOBA (*34*).

Step 4. The simulated progress curves corresponding to the mechanism depicted in **Schemes 1** and **2B** (**Figure 1** trace b), using the values of the kinetic constants described in the bibliography (*34, 37*), show how the rate at which DOBA, $V_0^{D,P}$, accumulates matches the rate of disappearance of the substrates V_0^D and $2V_0^{D,O_2}$ (**Table 2**).

Method 3: S_B. Step 1. Along the same lines as the mechanism of **Scheme 2B**, although with slight variations, **Scheme 2C** represents the kinetics of catecholamine oxidation by PPO.

Step 2. **Scheme 2C** describes the oxidation of substrate *o*-diphenol, which gives rise to a quinone (QH), which undergoes a process of deprotonation, passing to Q. This, in turn, is cyclized to leucoaminochrome, L, which is oxidized by QH, regenerating D and forming aminochrome, DC.

Table 2. Diphenolase Activity: Proposed Spectrophotometric Measurement Methods

method	substrate	coupled reagent	measurable species	λ (nm)	ϵ (M^{-1} cm^{-1})	V_0^D (nM s^{-1})	V_0^{D,O_2} (nM s^{-1})	$V_0^{D,P}$ (nM s^{-1})	refs
1	TBC (S_A)	none	Q	400	1200	−604	−302	604	*37*
2	DOMA (S_B)	none	DOBA	350	10500	−771	−385	771	*34*
3	L-dopa (S_B)	none	DC	475	3600	−233	−233	233	*26, 50, 58*
4	L-dopa (S_C)	MBTH	NQ	484	22300	−233	−233	233	*37*
5	TBC (S_A)	Cys	5-Cys-TBC	300	1598	−935	−467	935	*39*
6	CAT (S_D)	AH_2	AH_2	262	11170	≈0	−522	−1043	*44*
7	CAT (S_D)	AH_2	Q	400	1200	≈0	−515	1050	*44*
8	CAT (S_D)	AH_2	AH_2 + Q	250		≈0	−515	1050	*44*

The quantity of matter that enters the system in time t is V_0t, which is distributed in accordance with

$$V_0t = [QH] + [Q] + [DC] + [D]_R \quad (14)$$

where $[D]_R$ indicates the D generated from QH, which is equivalent to [DC], and so in the steady state

$$[DC] = \frac{V_0}{2}t - \frac{[QH]_{ss} + [Q]_{ss}}{2} \quad (15)$$

From eq 15, it can be affirmed that DC is accumulated in the steady state at a velocity corresponding to half the initial velocity of the enzyme's action.

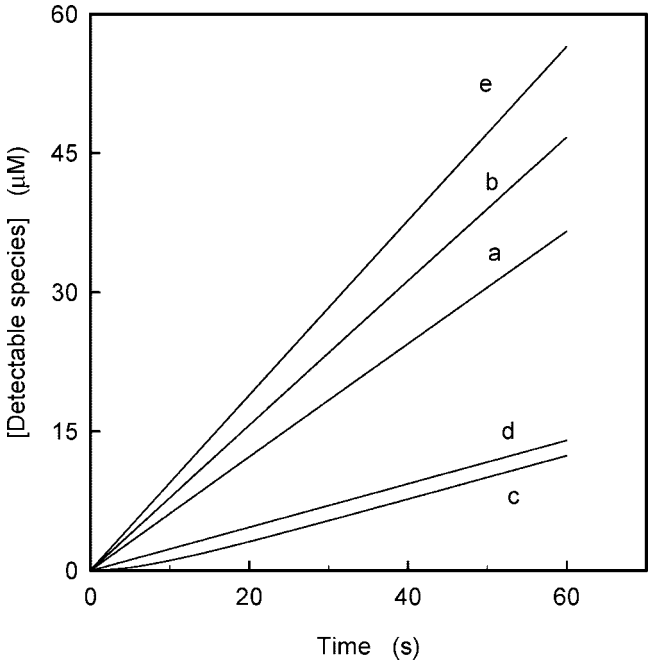

Figure 1. Action of PPO on different *o*-diphenols, types S_A, S_B, and S_C, methods 1–5. Curves obtained by simulation of a set of differential equations corresponding to each mechanism for the accumulation of each experimentally measurable species. Method 1 (**Schemes 1** and **2A**): substrate, TBC; measurable species, *o*-quinone (Q); trace a, the concentrations were $[O_2]_0 = 0.26$ mM, $[S]_0 = 2$ mM, $[E]_0 = 1$ nM. Method 2 (**Schemes 1** and **2B**): substrate, DOMA; measurable species, DOBA (P); trace b, the concentrations were $[O_2]_0 = 0.26$ mM, $[S]_0 = 5$ mM, $[E]_0 = 1$ nM. Method 3 (**Schemes 1** and **2C**): substrate, L-dopa; measurable species, dopachrome (DC); trace c, the concentrations were $[O_2]_0 = 0.26$ mM, $[S]_0 = 2$ mM, $[E]_0 = 2$ nM. Method 4 (**Schemes 1** and **2D**), substrate, L-dopa in the presence of MBTH; measurable species, nucleophile-quinone (NQ). Trace (d). The concentrations were $[O_2]_0 = 0.26$ mM, $[S]_0 = 2$ mM, $[E]_0 = 2$ nM. Method 5 (**Schemes 1** and **2E**): substrate, TBC in the presence of L-cysteine (N); measurable species, adduct (A); trace e, the concentrations were $[O_2]_0 = 0.26$ mM, $[S]_0 = 12$ mM, $[E]_0 = 1$ nM, $[N]_0 = 1.5$ mM.

Step 3. In this case, we should consider the oxidation of the catecholamines: L-dopa (*26*), dopamine (*27*), L-α-methylnoradrenaline (*28*), L-isoproterenol (*29*), and L-dopa methyl ester (*53*).

Step 4. The simulation of the reaction according to **Schemes 1** and **2C** according to the rate constants described in the bibliography (*48*) is reflected in **Figure 1** (trace c). According to eq 9, DC accumulates with a velocity of $V_0/2$. Therefore, with this method, the measurable velocity $V_0^{D,DC}$ is $V_0/2$. Note that the lag period depends on the rate constants of the different chemical *steps* (*26*). It is easy to demonstrate that the lag period follows the expression (*26*)

$$\tau = \frac{1}{2k_{app}} \quad (16)$$

where

$$k_{app} = \frac{k_{+d}k_c}{k_{-d}[H^+] + k_c} \quad (17)$$

The values obtained for the accumulation rate of DC ($V_0^{D,DC}$) and disappearance of D and O_2 (V_0^D and V_0^{D,O_2}) are equal (see **Table 2**). This analysis shows how spectrophotometric methods that measure the stable final product produced through the evolution of Q are suitable for obtaining reliable values of V_0. Furthermore, as we shall see below, the method permits us to characterize the monophenolase activity of PPO on the monophenols corresponding to these *o*-diphenols.

Method 4: S_B and S_C. Step 1. A variation of the mechanism shown in **Scheme 2C** consists of adding a nucleophile (N) to the medium to attack the Q generated by the enzyme, forming an adduct (A), which is oxidized by a molecule of Q originating the chromophore nucleophile-quinone (NQ) and regenerating D (**Scheme 2D**).

Step 2. The mass balance is equivalent to that of **Scheme 2C** and fulfills

$$[NQ] = \frac{V_0}{2}t - \frac{[Q]_{ss} + [A]_{ss}}{2} \quad (18)$$

In agreement with eq 18, the accumulation of [NQ] versus t gives a straight line with a slope $V_0/2$. This method has been used to characterize different substrates of PPO from several vegetal sources, melanoma, mushroom, and apple (*33, 35–38*). The nucleophile used was MBTH, which gives rise to a nucleophile-quinone with a high molar absorptivity (*37*).

Step 3. This method has been applied to study the oxidation of L-dopa by PPO. The recording was made at the wavelength of the isosbestic point (λ_i) corresponding to the evolution to NQ with its molar absorptivity of 22300 ± 500 M^{-1} cm^{-1} (*37*).

Step 4. The simulation of the mechanism of **Schemes 1** and **2D** shows that the accumulation of NQ, **Figure 1** (trace d), occurs at a velocity of $V_0/2$, and, in agreement with eq 18, $V_0/2$ $V_0^{D,NQ} = V_0/2$. This value $V_0^{D,NQ}$ is equivalent to the disappearance rate of the substrates V_0^D and V_0^{D,O_2} (**Table 2**). This method therefore can be considered rigorous and capable of obtaining correct values of V_0. Other authors have used L-proline as nucleophile (*32*).

Method 5: S_A, S_B, S_C, and S_D. Another possibility that has been used to obtain values of the diphenolase activity of PPO consists of attacking the *o*-quinone with L-cysteine (L-Cys), generating an adduct, 5-cysteinyl-diphenol (5-CysD) (*39*).

Step 1. The kinetic mechanism corresponding to this method is expressed in **Scheme 2E**.

Step 2. In this case the mass balance will be

$$V_0 t = [Q] + [5\text{-CysD}] \quad (19)$$

and so in the steady state

$$[5\text{-CysD}] = V_0 t - [Q]_{ss} \quad (20)$$

i.e., the accumulation of [5-CysD] versus t occurs with a velocity of V_0.

Step 3. This method has been applied experimentally with mushroom and apple tyrosinase (*39*).

Step 4. The simulation of **Scheme 2E** provides the curve shown in **Figure 1** (trace e), and in agreement with eq 20, its slope is $V_0 = V_0^{D,A}$. Note the closeness to the disappearance rate of D, V_0^D, and $V_0^{D,A}$ (**Table 2**) and thus $V_0 = V_0^{D,A} = V_0^D = 2V_0^{D,O_2}$. However, the molar absorptivity of 5-CysD does not represent an improvement over other methods (*39*). This method has the inconvenience that Cys inhibits many PPO, while the data obtained with apple PPO indicate that this enzyme is not inhibited by L-Cys at the concentrations used in the experiment (*39*).

Method 6: S_A, S_B, S_C, and S_D. This method, as well as methods 7 and 8 can be applied to all *o*-diphenols corresponding to substrates types S_A, S_B, S_C, and S_D. Spectrophotometric measurements can be made using ascorbic acid (AH_2), which reduces the *o*-quinones back to *o*-diphenols. Other authors have used NADH (*55*), which has a lower reduction potential than AH_2. The reaction can be followed in two ways, depending on whether the AH_2 spectrum is superimposed or not on that of the substrate.

For method 6, if the spectrum of the substrate is not superimposed on that of the AH_2, the disappearance of the ascorbic acid can be measured.

Step 1. The kinetic mechanism is the same as that described in **Scheme 2F**.

Step 2. According to the mass balance, the kinetic analysis indicates that the quantity of matter entering the system $V_0 t$ is distributed as follows

$$V_0 t = [Q] + [D]_R \quad (21)$$

The regenerated diphenol is $[D]_R$ and is equivalent to the amount of consumed $[AH_2]$, so that

$$V_0 t = [Q] + ([AH]_0 - [AH]_t) \quad (22)$$

The concentration of Q in the steady state is constant, so that the following is fulfilled:

$$\frac{d[Q]}{dt} = V_0 - k[Q]_{ss}[AH_2] = 0 \quad (23)$$

$$[Q]_{ss} = \frac{V_0}{k[AH_2]} \quad (24)$$

The concentration of AH_2 varies very little so that Q disappears with a pseudo-first-order constant k $[AH_2]$, which is very high, so that $[Q] \rightarrow 0$. In this way, according to eq 22

$$[AH_2]_0 - [AH_2]_t = V_0 t \quad (25)$$

so that by measuring the disappearance of AH_2 the initial velocity of the enzyme activity, V_0, can be determined. Note that in this method the disappearance of the coupled reagent and not of the substrate is followed. The method is applicable to any diphenol that does not show a spectrum overlapping that of the AH_2.

Step 3. This method has been applied to the oxidation of the catechol by tyrosinase. The slope corresponds to V_0 (*21, 44*).

Step 4. Numerical integration of the system of differential equations that correspond to the mechanism described in **Schemes 1** and **2E** provides the curve shown in **Figure 2** (trace a), the slope giving the value $V_0 = V_0^{D,AH_2}$. Note that no substrate (D) disappears until the AH_2 is consumed and V_0^{D,O_2} is half V_0^{D,AH_2} (**Table 2**).

Method 7: S_A, S_B, S_C, and S_D. If the spectra of the substrate and AH_2 overlap, another approach must be used. We call this the chronometric method since it consists of determining, by means of spectrophotometric recordings, the time that the enzyme acting on *o*-diphenols takes to consume a known quantity of AH_2.

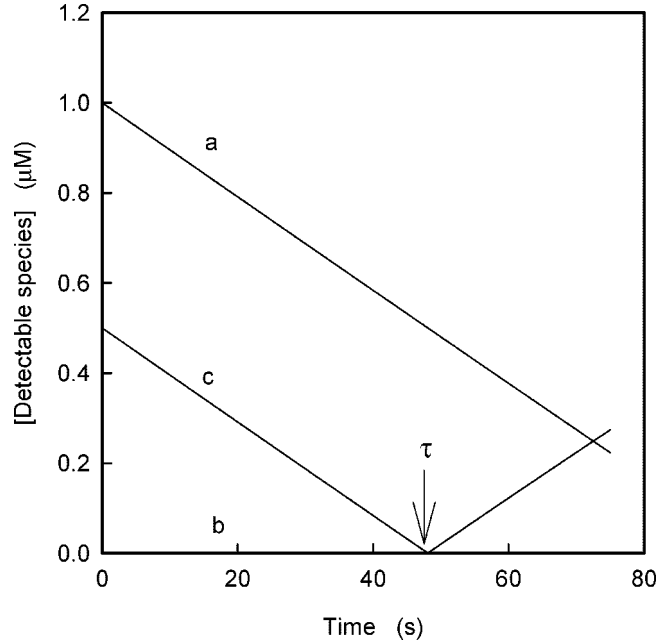

Figure 2. Action of PPO on a *o*-diphenol type S_D in presence of AH_2. Methods 6–8 (**Schemes 1** and **2F**): substrate CAT, curves obtained by simulation of a set of differential equations corresponding to mechanism of **Schemes 1** and **2F**. The concentrations were $[O_2]_0 = 0.26$ mM, $[S]_0 = 0.3$ mM, $[AH_2]_0 = 50$ μM (methods 7 and 8), $[AH_2]_0 = 100$ μM (method 6), and $[E]_0 = 1$ nM. Method 6: measurable species, ascorbic acid (AH_2) (trace a). Method 7: measurable species, Q (trace b). Method 8: the detectable signal is due to two measurable species, $AH_2 + Q$ (trace c).

Step 1. The kinetic scheme is that of **Scheme 2E**, but in this case the AH_2 is used up.

Step 2. The mass balance is

$$V_0 t = [Q] + [AH_2] \quad (26)$$

that is, the matter entering the system in the form of Q, $V_0 t$, consumes the AH_2 and, when no more AH_2 remains, Q is accumulated in the medium. A spectrophotometric record at the wavelength at which Q is absorbed shows that there is a lag period (τ) since Q is reduced to D. The prolongation of the accumulation of Q intercepts the time axis at $t = \tau$ and, according to eq 26, if $[Q] = 0$, then

$$V_0 \tau = [AH_2]_0 \quad (27)$$

and therefore

$$V_0 = \frac{[AH_2]_0}{\tau} \quad (28)$$

Step 3. This method has been applied experimentally to the kinetic characterization of several PPO substrates (*44*).

Step 4. Simulation of the set of differential equations defining **Schemes 1** and **2E** provides the recording, **Figure 2** (trace b) with its lag period, τ, from which V_0 can be obtained. The disappearance rate of the substrate V_0^D is zero and $V_0 = V_0^{D,AH_2}$ and V_0^{D,O_2} is half, in agreement with the stoichiometry (**Table 2**) (*48*).

Method 8: S_A, S_B, S_C, and S_D. This method is based on the consumption of a given quantity of AH_2, measuring its disappearance from the spectrophotometric signal. As the AH_2 is being consumed, the signal diminishes, and when the AH_2 has been totally used up, the signal begins to rise as a result of the increased absorbance of the *o*-quinone, so that there is an inflection in the signal. The critical point of the change in direction of the spectrophotometric signal corresponds

to the time, τ, that AH_2 takes to be consumed. We call this method the alternative chronometric method (*44*).

Step 1. The mechanism is described by **Scheme 2E**.

Step 2. The kinetic analysis is the same as that of method 7.

Step 3. This method has recently been applied to studying the reaction of catechol with mushroom PPO (*44*).

Step 4. The simulation of the mechanism of **Schemes 1** and **2E** in which $[AH_2] + [Q]$ is represented shows a curve as described in **Figure 2** (trace c). The value of V_0, obtained from τ, is shown in **Table 2** and agrees with the substrate disappearance rate, V_0^{D,O_2} (see **Table 2**).

In conclusion, for the diphenolase activity of PPO, we have analyzed a series of spectrophotometric methods (methods 1–8) that measure (i) the direct product of the action of the enzyme, the *o*-quinone (method 1), (ii) some compound derived from its evolution (methods 2–5), or (iii) the reduction of *o*-quinone by AH_2 (methods 6–8). In all cases, it is shown that the short time measurements made in the steady state are valid and equivalent to measuring the disappearance of substrate, in agreement with the stoichometry of the reaction (**Table 2**).

Monophenolase Activity. The action mechanism of PPO on monophenols is depicted in **Scheme 3** (*50*). Note that the monophenolase activity is coupled to the diphenolase activity and the series of chemical reactions that occurs after the formation of *o*-quinone and which generates *o*-diphenol in the medium (**Schemes 4A**, **4B**, and **4C**). Thus for monophenolase activity to occur, the reactions of **Scheme 3** must be fulfilled. For the measurement of monophenolase activity to be correct, regardless of the method used, the system must have reached the steady state. This steady state is reached if (a) the substrates monophenol and O_2 hardly vary and (b) the evolution of *o*-quinone to the chromophoric product is fast and with a clear stoichiometry, generating *o*-diphenol in the medium.

If these conditions are fulfilled, the quantity of matter entering the system will be the same as that leaving it and so

$$V_0 = -\frac{d[M]}{dt} = \frac{d[DC]}{dt} \tag{29}$$

As regards **Scheme 3**, the analytical expression of the steady-state rate is

$$V_0^{M,DC} = \frac{V_{max}^{M,DC}[M]_0[O_2]_0}{K_m^M K_s^{O_2} + K_m^{O_2(M)}[M]_0 + K_m^M[O_2]_0 + [M]_0[O_2]_0} \tag{30}$$

with

$$V_{max}^{M,DC} = k_{cat}^M[E]_0 = \frac{k_{5_1}k_{5_2}}{k_{5_1} + k_{5_2}}[E]_0 \tag{31}$$

$$k_{cat}^M = \frac{k_{5_1}k_{5_2}}{k_{5_1} + k_{5_2}} \tag{32}$$

$$K_m^M = \frac{k_{cat}^M}{k_4} \tag{33}$$

$$K_m^{O_2(M)} = \frac{3k_{cat}}{2k_8} \tag{34}$$

Below we shall consider the four types of substrates, S_A, S_B, S_C, and S_D.

Method 9: S_A. Step 1. The mechanism with stable *o*-quinone can be represented as in **Scheme 3** (*56*).

Step 2. The kinetic analysis of this mechanism shows that the system never reaches the steady state and therefore V_0 cannot be determined correctly (*52*).

Step 3. When the oxidation of TBF by PPO was studied (*52*), it was seen that the rate diminished as substrate concentration increased, which agrees with what was said about step 2, and so eq 30 is not fulfilled (*52*).

Step 4. The numerical integration of the system of differential equations corresponding to the mechanism of **Scheme 3** is shown in

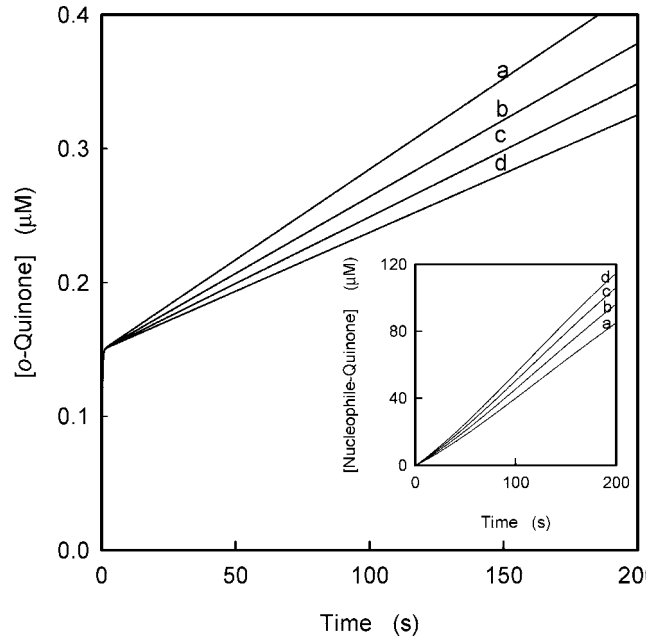

Figure 3. Action of PPO on type S_A monophenols that originate stable *o*-quinones. Method 9 (measurable species, *o*-quinone) and method 11 in presence of MBTH (measurable species, nucleophile-quinone). Curves obtained by simulation of set of differential equations corresponding to each mechanism. method 9: substrate TBF (**Scheme 3** with $D = 0$), measurable species, *o*-quinone (Q). The concentrations were $[O_2]_0 = 0.26$ mM, $[S]_0$, (a) 0.5 mM, (b) 0.6 mM, (c) 0.7 mM, (d) 0.8 mM, $[E]_0 = 10$ nM. Method 11: substrate 4-HA, in the presence of MBTH (**Schemes 3** and **4B**), measurable species, nucleophile-quinone (QN). The concentrations were $[O_2]_0 = 0.26$ mM, $[S]_0$, (a) 0.5 mM, (b) 0.6 mM, (c) 0.7 mM, (d) 0.8 mM, $[E]_0 = 20$ nM.

Figure 3. Note how, the apparent steady-state rate decreases as the substrate concentration increases (*52*, *56*).

The above results lead us to conclude that these monophenols cannot be characterized and so measurement method 9 is not valid. As will be shown below, in the case of 4-hydroxyanisole, 4HA, the evolution of the *o*-quinone observed is provoked with a nucleophile-like MBTH (*57*), although, this is not possible in the case of TBF because the *o*-quinone is less reactive.

Method 10: S_B. Among this group are L-tyrosine (*40*), tyramine, and L-tyrosine methyl ester (*53*), for which we propose the following measurement method.

Step 1. The kinetic mechanism reflecting this method is described in **Scheme 4A**. The enzyme attacks monophenol, converting it to *o*-diphenol. This gives rise to QH, which is deprotonated. It cyclized to leukodopachrome, L, and it is oxidized by QH, forming D and DC (*40*, *53*, *58*).

Step 2. The mass balance for the mechanism of **Scheme 3B** in the steady state establishes

$$V_0^{M,DC}t = [DC] + [I]_{ss} \tag{35}$$

where $V_0^{M,DC}$ is the initial rate of tyrosinase action on monophenol, DC represents aminochrome, and $[I]_{ss}$ indicates the intermediate products that accumulate in the steady state.

Rearranging eq 35, it becomes

$$[DC] = V_0^{M,DC}t - [I]_{ss} \tag{36}$$

The slope of the straight line in the steady state is $V_0^{M,DC}$.

Step 3. This method has been used experimentally to characterize several catecholamines (*26–29*, *31*, *40*, *53*).

Step 4. Simulation of the set of differential equations that represent the mechanism of **Schemes 3** and **4A** gives the initial rate of DC accumulation in the steady state, **Figure 4** (trace a). **Table 3** shows

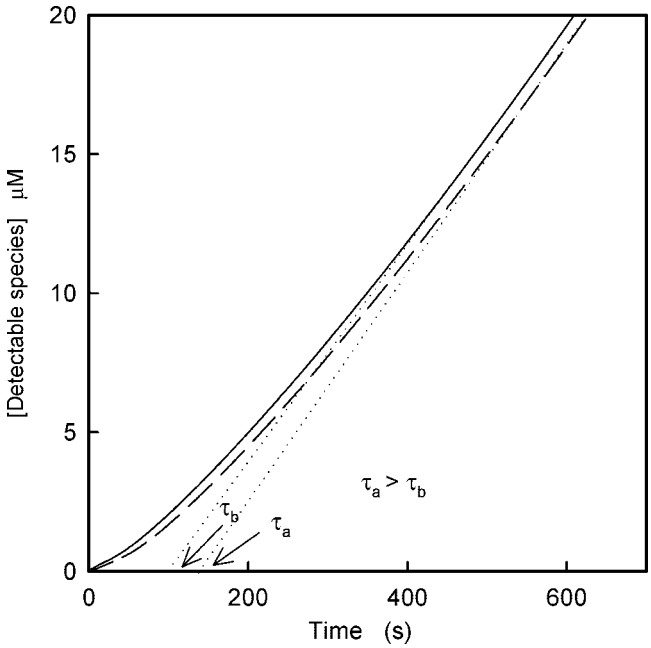

Figure 4. Action of PPO on different types of S_B and S_C monophenols. Methods 10 and 11, curves obtained by simulation of set of differential equations corresponding to each mechanism. Method 10: substrate L-tyrosine (**Schemes 3** and **4A**), measurable species aminochrome DC, trace a. The concentrations were $[O_2]_0 = 0.26$ mM, $[S]_0 = 2$ mM, $[E]_0 = 25$ nM. Method 11: substrate L-tyrosine in the presence of MBTH (**Scheme 3** and **4B**), measurable species, nucleophile-quinone, (NQ), trace b. The concentrations were the same as in method 10.

the value $V_0^{M,DC}$, which agrees with the disappearance rate of monophenol and O_2, V_0^M and V_0^{M,O_2}, according to the reaction stoichiometry in (*50*).

Method 11: S_B and S_C. Step 1. The mechanism is that of **Scheme 4B**.

Step 2. The kinetic analysis of the mechanism of **Scheme 4B** is similar to that of **Scheme 4A**, the following mass balance being fulfilled in the steady state:

$$V_0^{M,NQ}t = [NQ] + [I]_{ss} \quad (37)$$

Rearranging eq 37 gives the straight line representing NQ accumulation, according to

$$[NQ] = V_0^{M,NQ}t - [I]_{ss} \quad (38)$$

The slope of this line gives $V_0^{M,NQ}$, the steady-state rate.

Step 3. This method has been applied experimentally to the kinetic characterization of several PPO substrates from different sources (*32, 33, 35–38, 59*).

Step 4. A numerical integration of the system of differential equations that represents the mechanism of **Schemes 3** and **4B**, taking into account the values of the kinetic constants available in the bibliography (*37*), gives the curve of **Figure 4** (trace b). The values of the appearance rate of NQ, $V_0^{M,NQ}$, and the disappearance rate of M and O_2, V_0^M and V_0^{M,O_2}, respectively, are shown in **Table 3**. When the kinetics of the oxidation of 4HA in the presence of MBTH is simulated, similar behavior is observed (**Figure 3** inset), because, despite its stability, the *o*-quinone of 4HA is capable of reacting with MBTH in accordance with **Scheme 4B** (*37, 57*).

Method 12: S_D. In the case of diphenolase activity, the S_D substrates can be studied in the presence of AH_2 (methods 6–8). However, the presence of AH_2 (in the case of monophenolase activity) hinders the measurement because *o*-diphenol is continuously accumulated in the medium and so the system does not reach its steady state.

Step 1. The mechanism is that depicted in **Scheme 4C**. Note that in this case all the *o*-quinone is reduced to *o*-diphenol, which accumulates constantly in the medium.

Step 2. There is no analytical solution in the steady state for this mechanism since it is never reached.

Step 3. The experimental recordings of O_2 consumption are shown in (*51*), where the parabolic decrease in O_2 concentration indicates that the steady state has not been reached.

Step 4. The simulation mechanism of **Schemes 3** and **4C** is shown in **Figure 5** and agrees with the experimental recordings of (*51*). **Table 3** shows that the rates in the presence of AH_2 (method 12) are higher than in its absence (method 10).

The results suggest that monophenolase activity can be characterized if the system reaches the steady state. For this to happen *o*-diphenol recycling must occur in the medium, although it cannot be a constant process as it is in methods 10 and 11. For the four types of substrate described (S_A–S_D) the following can be established:

CONCLUSIONS

The present work discusses several spectrophotometric methods for kinetically characterizing a series of monophenols and diphenols acting as PPO substrates. The methods that measure the appearance of a product and its evolution to a stable chromatophoric compound or the disappearance of AH_2 as coupled reagent show clear advantages over methods that measure substrate disappearance. Through analytical solutions and simulation, we have shown that as long as there is a clear stoichiometry in the evolution of the product of an enzymatic reaction, the initial velocity of the enzyme can be estimated measuring the final stable compound.

The difficulty of measuring monophenols compared with diphenols is clear. Type S_A, S_B, S_C, and S_D diphenolic substrates can be characterized, while in the case of monophenolic substrates, only types S_B and S_C can be studied kinetically.

For S_A substrates of diphenolase activity the best method is method 1. For types S_B and S_C whose *o*-quinones react

Table 3. Monophenolase Activity: Proposed Spectrophotometric Measurement Methods[a]

method	substrate	coupled reagent	measurable species	λ (nm)	ε (M^{-1} cm^{-1})	V_0^M (nM s^{-1})	V_0^{M,O_2} (nM s^{-1})	F (nM s^{-1})	refs
9	TBF[1] (S_A)	none	Q	400	1237	−1.34	−1.34	1.34	*52, 56*
9	TBF[2] (S_A)	none	Q	400	1237	−1.14	−1.14	1.14	*52, 56*
9	TBF[3] (S_A)	none	Q	400	1237	−0.99	−0.99	0.99	*52, 56*
9	TBF[4] (S_A)	none	Q	400	1237	−0.87	−0.87	0.87	*52, 56*
11	4HA[1] (S_C)	MBTH	NQ	459	19230	−415	−622	415	*35, 37*
11	4HA[2] (S_C)	MBTH	NQ	459	19230	−460	−687	460	*35, 37*
11	4HA[3] (S_C)	MBTH	NQ	459	19230	−487	−730	487	*35, 37*
11	4HA[4] (S_C)	MBTH	NQ	459	19230	−500	−749	500	*35, 37*
10	Tyr (S_B)	none	DC	480	3300	−56	−82	54	*58*
12	Tyr (S_C)	MBTH	NQ	476	20700	−56	−82	54	*37*
10	Tyr+(S_B)	None	DC	475	3600	−35.1	−52.6	35	*58*
14	Tyr+(S_D)	AH_2	AH_2	262	11170	−33.2	−162	−291	this paper

[a] [TBF] and [4HA] were (1) 0.5 mM, (2) 0.6 mM, (3) 0.7 mM, and (4) 0.8 mM. [Tyr] (+) was 0.25 mM.

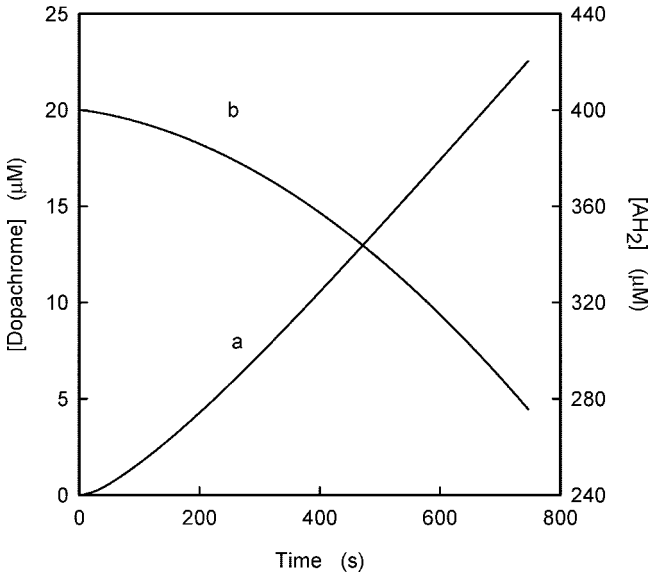

Figure 5. Action of PPO on monophenols in absence and presence of AH_2, methods 10 and 12, respectively. Curves obtained by simulation of set of differential equations corresponding to method 10: substrate L-tyrosine, (**Scheme 3** and **4A**). The concentrations are $[O_2]_0 = 0.26$ mM, $[E]_0 = 25$ nM, trace a, $[S]_0 = 0.25$ mM. Method 12: substrate L-tyrosine in the presence of AH_2 (**Scheme 3** and **4C**). $[AH_2]_0 = 400$ μM, trace b, $[S]_0 = 0.25$ mM.

with MBTH, the must appropriate method is method 4 due to the high molar absorptivity and stability of the NQ adduct. In the case of type S_D substrates, depending on the extent to which the S_D and AH_2 spectra overlap, methods 6–8 can be chosen.

Methods 9 and 12 are of no use for determining monophenolase activity because the system does not reach steady state. Substrate S_C can only be measured by method 11. The best way to measure substrate S_B is method 11 due to the high molar absorptivity and stability of the NQ adduct.

Finally, it is convenient to unify the definition of the international units used in the assays and to establish a relationship between diphenolase and monophenolase activity units (*61*).

NOTATIONS AND DEFINITIONS

Enzymatic species

E	enzyme, PPO
$[E]_0$	initial PPO concentration
E_d	*deoxy*tyrosinase (with Cu^+–Cu^+ in the active site)
E_m	*met*tyrosinase (with Cu^{2+}–Cu^{2+} in the active site)
E_mD	*met*tyrosinase *o*-diphenol binding complex
E_mM	*met*tyrosinase monophenol binding complex
E_{ox}	*oxy*tyrosinase (Cu^{2+}–O_2^{2-}–Cu^{2+} in the active site)
$E_{ox}D$	*oxy*tyrosinase *o*-diphenol binding complex
$E_{ox}M$	*oxy*tyrosinase monophenol binding complex
E_{ox}-M	covalently bound *oxy*tyrosinase monophenol
PPO	polyphenol oxidase or tyrosinase

Substrates

CAT	catechol
D	*o*-diphenol
$[D]_{ss}$	steady-state concentration of D
DOMA	3,4-dihydroxymandelic acid
4HA	4-hydroxyanisole
M	monophenol
S	substrate
TBC	4-*tert*-butylcatechol
TBF	4-*tert*-butylphenol
L-Tyr	L-tyrosine
$[X]_0$	initial concentration of the substrate X

Coupled reagents and concentrations

AH_2	ascorbic acid
Cys	L-cysteine
MBTH	3-methyl-2-benzothiazoline hydrazone
N	nucleophilic reagent
Pro	proline
$[R]_0$	initial concentration of the reagent R

Products

CysD	cysteinyldiphenol
DC	dopachrome
DOBA	3,4-dihydroxybenzaldehyde
NQ	nucleophile-quinone
o-TBQ	*o*-*tert*-butylquinone
P	product
Q	*o*-quinone

Kinetic parameters

V_0	initial rate of PPO acting on a substrate, equivalent to V_{ss}, steady-state rate
$V_0^{S,X}$	steady-state rate of the diphenolase (S = D) or monophenolase (S = M) activity of PPO, measuring the disappearance of the substrate X, or the appearance of the product X
V_0^S	steady-state rate of the diphenolase (S = D) or monophenolase (S = M) activity of PPO, measuring the disappearance of D or M
τ	lag period

Kinetic constants

K_i	rate constants
K_N	nucleophilic attack constant
K_c	cyclization constant
K_{+d}	deprotonation constant
K_{-d}	protonation constant
K_R	oxidation–reduction constant
K_{app}	apparent constant of *o*-quinone transformation into aminochrome or nucleophile-quinone
K_m^S	Michaelis constant of PPO for D (S = D) or M (S = M)
$K_s^{O_2}$	disociation constant of the O_2 of E_{ox}
$K_m^{O_2S}$	Michaelis constant for O_2 in presence of D (S = D) or M (S = M)
K_{cat}^S	catalytic constant for PPO in presence of D (S = D) or M (S = M)
V_{max}^S	maximum velocity for PPO in presence of D (S = D) or M (S = M)

Supporting Information Available: Sets of differential equations that correspond to each measuring method. This material is available free of charge via the Internet at http://pubs.acs.org.

LITERATURE CITED

(1) Prota, M. G.; d'Ischia, A.; Napolitano, A. In *The Pigmentary System*; Nordlund, J. J.; Boissy, R., Hearing, V., King, R., Ortonne, J. P., Eds.; University Press: Oxford, 1988.

(2) Solomon, E. I.; Sundaram, U. M.; Machonkin, T. E. Multicopper

oxidases and oxygenases. *Chem. Rev.* **1996**, *96*, 2563–2606.
(3) Jaenicke, E.; Decker, H. Functional changes in the family of type 3 copper proteins during evolution. *ChemBioChem* **2004**, *5*, 163–169.
(4) Solomon, E. I.; Chen, P.; Metz, M.; Lee, S. K.; Palmer, A. E. Oxygen binding, activation, and reduction to water by copper proteins. *Angew. Chem., Int. Ed.* **2001**, *40*, 4570–4590.
(5) Magnus, K. A.; Hazes, B.; Ton-That, H.; Bonaventura, C.; Bonaventura, J.; Hol, W. G. Crystallographic analysis of oxygenated and deoxygenated states of arthropod hemocyanin shows unusual differences. *Proteins* **1994**, *19*, 302–309.
(6) Cuff, M. E.; Miller, K. I.; van Holde, K. E.; Hendrickson, W. A. Crystal structure of a functional unit from *Octopus* hemocyanin. *J. Mol. Biol.* **1998**, *278*, 855–870.
(7) Klabunde, T.; Eicken, C.; Sacchettini, J. C.; Krebs, B. Cristal structure of a plant catechol oxidase containing a dicopper center. *Nat. Struct. Biol.* **1998**, *5*, 1084–1090.
(8) Bubacco, L.; Salgado, J.; Tepper, A. W.; Vijgenboom, E.; Canters, G. W. ^{1}H NMR spectroscopy of the binuclear Cu(II) active site of *Streptomyces antibioticus* tyrosinase. *FEBS Lett.* **1999**, *442*, 215–222.
(9) Matoba, Y.; Kumagai, T.; Yamamoto, A.; Yoshitsu, H.; Sugiyama, M. Crystallographic evidence that the dinuclear cooper center of tyrosinase is flexible during catalysis. *J. Biol. Chem.* **2006**, *281*, 8981–8990.
(10) Yoruk, R.; Marshall, M. R. Physiochemical properties and function of plant polyphenol oxidase: a review. *J. Food Chem.* **2003**, *27*, 361–422.
(11) Seo, S. Y.; Sharma, V. K.; Sharma, N. Mushroom tyrosinase: recent prospects. *J. Agric. Food. Chem.* **2003**, *51*, 2873–2853.
(12) Mayer, A. M. Polyphenol oxidases in plants and fungi: Going places? A review. *Phytochemistry* **2006**, *67*, 2318–2331.
(13) Halaouli, S.; Asther, M.; Sigoillot, J. C.; Hamdi, M.; Lomascolo, A. Fungal tyrosinases: new prospects in molecular characteristics bioengineering and biotechnological applications. *J. Appl. Microbiol.* **2006**, *100*, 219–232.
(14) Nicolas, J. J.; Richard-Forget, F. C.; Goupy, P. M.; Amiot, M. J.; Auber, S. Y. Enzymatic browing reactions in apple and apple products. *Crit. Rev. Food Sci. Nutr.* **1994**, *34*, 109–157.
(15) Pomerantz, S. H. The tyrosine hydroxylase activity of mammalian tyrosinase. *J. Biol. Chem.* **1966**, *241*, 161–168.
(16) Pomerantz, S. H. A sensitive new assay for the oxidation of 3,4-dihydroxy-L-phenylalanine by tyrosinase. *Anal. Biochem.* **1976**, *75*, 86–90.
(17) Rodriguez-López, J. N.; Ros Martinez, J. R.; Varón, R.; García-Cánovas, F. Calibration of a clark-type oxygen electrode by tyrosinase-catalyzed oxidation of 4-*tert*-butylcatechol. *Anal. Biochem.* **1992**, *202*, 356–360.
(18) Solano-Muñoz, F.; Peñafiel, R.; Galindo, J. D. An electrometric method for the determination of tyrosinase activity. *Biochem. J.* **1985**, *229*, 573–578.
(19) Miller, H. W.; Dawson, C. R. A new method for the measurement of tyrosinase catecholase activity. *J. Am. Chem. Soc.* **1941**, *63*, 3375–3382.
(20) Miller, H. W.; Mallette, M. F.; Roth, L. J.; Dawson, C. R. A new method for the measurement of tyrosinase catecholase activity II, catecholase activity based on the initial reaction velocity. *J. Am. Chem. Soc.* **1944**, *66*, 514–519.
(21) El-Bayoumi, M. A.; Frieden, E. A spectrophotometric method for the determination of the catecholase activity of tyrosinase and some of its applications. *J. Am. Chem. Soc.* **1957**, *79*, 4854–4858.
(22) Pifferi, P. G.; Baldassari, L. A spectrophotometric method for the determination of the cathecholase activity of tyrosinase by Besthorn's hydrazone. *Anal. Biochem.* **1973**, *52*, 325–335.
(23) Pifferi, P. G.; Baldassari, L.; Cultrera, R. Inhibition by carboxylic acids of an *o*-diphenol oxidase from *Prunus avium* fruits. *J. Sci. Food Agric.* **1974**, *25*, 263–270.
(24) Mazzocco, F.; Pifferi, P. G. An improvement of the spectrophotometric method for the determination of tyrosinase catecholase activity by Besthorn's hydrazone. *Anal. Biochem.* **1976**, *72*, 643–647.
(25) García-Carmona, F.; Pedreño, E.; Galindo, J. D.; García-Cánovas, F. A new spectrophotometric method for the determination of cresolase activity of epidermis tyrosinase. *Anal. Biochem.* **1979**, *95*, 433–435.
(26) García-Carmona, F.; García-Cánovas, F.; Iborra, J. L.; Lozano, J. A. Kinetic study of the pathway of melanization between L-dopa and dopachrome. *Biochim. Biophys. Acta* **1982**, *717*, 124–131.
(27) Jiménez, M.; García-Carmona, F.; García-Cánovas, F.; Iborra, J. L.; Lozano, J. A.; Martinez, F. Chemical intermediates in dopamine oxidation by tyrosinase and kinetic study of the process. *Arch. Biochem. Biophys.* **1984**, *235*, 438–448.
(28) Jiménez, M.; García-Carmona, F.; García-Cánovas, F.; Iborra, J. L.; Lozano, J. A. Chemical intermediates in L-α-methylnoradrenaline oxidation by tyrosinase II. Kinetic study of the process. *Int. J. Biochem. Cell Biol.* **1985**, *17*, 891–894.
(29) Jiménez, M.; García-Cánovas, F.; García-Carmona, F.; Iborra, J. L.; Lozano, J. A. Isoproterenol oxidation by tyrosinase. Intermediates characterization and kinetic study. *Biochem. Int.* **1985**, *11*, 51–59.
(30) Vachtenheim, J.; Duchon, J.; Matous, B. A spectrophotometric assay for mammalian tyrosinase utilizing the formation of melanochrome from L-dopa. *Anal. Biochem.* **1985**, *146*, 405–410.
(31) Escribano, J.; García, M.; García-Cánovas, F.; García-Carmona, F.; Varón, R.; Tudela, J.; Lozano, J. A. Kinetic study of the transient phase of a chemical reaction system coupled to an enzymatically catalized step: Application to the oxidation of epinine by tyrosinase. *Biophys. Chem.* **1987**, *27*, 15–25.
(32) Rzepecki, L. M.; Waite, J. H. A chromogenic assay for catecholoxidases based on the addition of L-proline to *o*-quinones. *Anal. Biochem.* **1989**, *179*, 375–381.
(33) Winder, A. J.; Harris, H. New assays for the tyrosine hydroxylase and dopa oxidase activities of tyrosinase. *Eur. J. Biochem.* **1991**, *198*, 317–326.
(34) Rodríguez-Lopez, J. N.; Serna Rodríguez, P.; Tudela, J.; Varon, R.; García-Cánovas, F. A continuous spectrophotometric method for the determination of diphenolase activity of tyrosinase using 3,4-dihydroxymandelic acid. *Anal. Biochem.* **1991**, *195*, 369–374.
(35) Espín, J. C.; Varón, R.; Tudela, J.; García-Cánovas, F. Kinetic study of the oxidation of 4-hydroxyanisole catalyzed by tyrosinase. *Biochem. Mol. Biol. Int.* **1997**, *41*, 1265–1276.
(36) Winder, A. J. A stopped spectrophotometric assay for the dopa oxidase activity of tyrosinase. *J. Biochem. Biophys. Methods* **1994**, *28*, 173–183.
(37) Espín, J. C.; Varón, R.; Fenoll, L. G.; Gilabert, M. A.; García-Ruiz, P. A.; Tudela, J.; García-Cánovas, F. Kinetic characterization of the substrate specificity and mechanism of mushroom tyrosinase. *Eur. J. Biochem.* **2000**, *267*, 1270–1279.
(38) Espín, J. C.; García-Ruiz, P. A.; Tudela, J.; García-Cánovas, F. Study of the stereospecificity of pear and strawberry polyphenol oxidases. *J. Agric. Food Chem.* **1998**, *46*, 2469–2473.
(39) Gauillard, F.; Richard-Forget, F.; Nicolas, J. New spectrophotometric assay for polyphenol oxidase activity. *Anal. Biochem.* **1993**, *215*, 59–65.
(40) Fenoll, L. G.; Rodríguez-López, J. N.; García-Sevilla, F.; García-Ruiz, P. A.; Varón, R.; García-Cánovas, F.; Tudela, J. Analysis and interpretation of the action mechanism of mushroom tyrosinase on monophenols and diphenols generating highly unstable *o*-quinones. *Biochim. Biophys. Acta* **2001**, *1548*, 1–22.
(41) Behbahani, I.; Miller, S. A.; O'Keeffe, D. H. A comparison of mushroom tyrosinase dopaquinone and dopachrome assays using diode-array spectrophotometric; dopachrome formation vs a ascorbate-linked dopaquinone reduction. *Microchem. J.* **1993**, *47*, 251–260.
(42) Park, Y. D.; Lee, J. R.; Park, K. H.; Hah, H. S.; Hahn, M. J.; Yang, J. M. A new continuous spectrophotometric assay method for dopa oxidase activity of tyrosinase. *J. Protein Chem.* **2003**, *22*, 473–480.
(43) Haghbeen, K.; Tan, E. W. Direct spectrophotometric assay of monooxygenase and oxidase activities of mushroom tyrosinase in the presence of synthetic and natural substrates. *Anal. Biochem.* **2003**, *312*, 23–32.

(44) Muñoz, J. L.; Garcia Molina, F.; Varón, R.; Rodríguez-Lopez, J. N.; García-Cánovas, F.; Tudela, J. Calculating molar absorptivities for quinones: application to the measurement of tyrosinase activity. *Anal. Biochem.* **2006**, *351*, 128–138.
(45) Solano, F.; García-Borrón, J. C. Advances in Enzymatic Analysis of Melanogenesis. In *The Pigmentary System, physiology and Patophysiology*; Nordlund, J. J., Ed.; Oxford University Press: New York, 1998; pp 467–471.
(46) Segel, I. H. Kinetics of unireactant enzymes. In *Enzyme kinetics. Behaviour and analysis of rapid equilibrium and steady-state enzyme systems*; J. Wiley and Sons: London, 1975; p 83.
(47) Duckworth, H. W.; Coleman, J. E. Physicochemical and kinetic properties of mushroom tyrosinase. *J. Biol. Chem.* **1970**, *245*, 1613–1625.
(48) Rodriguez-Lopez, J. N.; Fenoll, L. G.; Garcia-Ruiz, P. A.; Varon, R.; Tudela, J.; Thorneley, R. N.; García-Cánovas, F. Stopped-flow and steady-state study of the diphenolase activity of mushroom tyrosinase. *Biochemistry* **2000**, *39*, 10497–10506.
(49) Fenoll, L. G.; Peñalver, M. J.; Rodríguez-López, J. N.; Varón, R.; García-Cánovas, F.; Tudela, J. Tyrosinase kinetics: discrimination between two models to explain the oxidation mechanism of monophenol and diphenol substrates. *Int. J. Biochem. Cell Biol.* **2004**, *36*, 235–246.
(50) Peñalver, M. J.; Fenoll, L. G.; Rodríguez-López, J. N.; García-Ruíz, P. A.; García-Molina, F.; Varón, R.; García-Cánovas, F.; Tudela, J. Reaction mechanism to explain the high kinetic autoactivation of tyrosinase. *J. Mol. Catal. B: Enzym.* **2005**, *33*, 35–42.
(51) Ros, J. R.; Rodriguez-Lopez, J. N.; García-Cánovas, F. Effect of L-ascorbic acid on the monophenolase activity of tyrosinase. *Biochem. J.* **1993**, *295*, 309–12.
(52) Ros, J. R.; Rodriguez-Lopez, J. N.; Varon, R.; García-Cánovas, F. Kinetic study of the oxidation of 4-*tert*-butylphenol by tyrosinase. *Eur. J. Biochem.* **1994**, *222*, 449–452.
(53) Fenoll, L. G.; Rodriguez-Lopez, J. N.; Varón, R.; García-Ruíz, P. A.; García-Cánovas, F.; Tudela, J. Kinetic characterization of the reaction mechanism of mushroom tyrosinase on tyramine/dopamine and L-tyrosine methyl esther/L-dopa methyl esther. *Int. J. Biochem. Cell Biol.* **2002**, *34*, 1594–1607.
(54) Garcia-Molina, F.; Peñalver, M. J.; Fenoll, L. G.; Rodriguez-Lopez, J. N.; García-Cánovas, F.; Tudela, J. Kinetic study of monophenol and *o*-diphenol binding to oxytyrosinase. *J. Mol. Catal. B: Enzym.* **2005**, *32*, 185–192.
(55) Brown, R. S.; Male, K. B.; Luong, J. H. A substrate recycling assay for phenolic compounds using tyrosinase and NADH. *Anal. Biochem.* **1994**, *222*, 131–139.
(56) Fenoll, L. G.; Rodriguez-Lopez, J. N.; García-Sevilla, F.; Tudela, J.; García-Ruiz, P. A.; Varón, R.; García-Cánovas, F. Oxidation by mushroom tyrosinase of monophenols generating slighty unstable *o*-quinones. *Eur. J. Biochem.* **2000**, *267*, 5865–5878.
(57) Espín, J. C.; Tudela, J.; García-Cánovas, F. 4-Hydroxianisole: The most suitable monophenolic substrate for determining spectrophotometrically the monophenolase activity of polyphenol oxidase from fruits and vegetables. *Anal. Biochem.* **1998**, *259*, 118–126.
(58) Ros, J. R.; Rodriguez-Lopez, J. N.; García-Cánovas, F. Tyrosinase: kinetic analysis of the transient phase and the steady-state. *Biochim. Biophys. Acta* **1994**, *1204*, 33–42.
(59) Espín, J. C.; García-Ruíz, P. A.; Tudela, J.; Varón, R.; García-Cánovas, F. Monophenolase and diphenolase reaction mechanisms of apple and pear polyphenol oxidases. *J. Agric. Food Chem.* **1998**, *46*, 2968–2975.
(60) García-Sevilla, F.; Garrido del Solo, C.; Duggleby, R. G.; García-Cánovas, F.; Peyro, R.; Varón, R. Use of a windows program for simulation of the progress curves of reactants and intermediates involved in enzyme-catalyzed reactions. *Biosystems* **2000**, *54*, 151–164.
(61) Fenoll, L. G.; Rodríguez-Lopez, J. N.; García-Molina, F.; García-Cánovas, F.; Tudela, J. Unification for the expresión of the monophenolase and diphenolase activities of tyrosinase. *IUBMB Life* **2002**, *54*, 137–141.

Received for review April 26, 2007. Revised manuscript received September 12, 2007. Accepted September 19, 2007. This work was supported in part by grants from the MEC (Spain) Project BIO 2006-15363, from the Consejería de Educación (BioCARM, Murcía) Project BIO-BMC 06/01-0004, and from the Fundación Séneca (CARM, Murcia) Project 00672/PI/04. F.G.-M. has a fellowship from the MEC (Spain), Reference AP2003-0891. J.L.M. has a fellowship from the MEC (Spain), Reference AP2005-4721.

JF0712301